

MULTIWAVE SIBERIAN RADIOHELIOGRAPH

A.T. Altyntsev

*Institute of Solar-Terrestrial Physics SB RAS,
Irkutsk, Russia, altyntsev@iszf.irk.ru*

S.V. Lesovoi

*Institute of Solar-Terrestrial Physics SB RAS,
Irkutsk, Russia, svlesovoi@gmail.com*

M.V. Globa

*Institute of Solar-Terrestrial Physics SB RAS,
Irkutsk, Russia, globa@iszf.irk.ru*

A.V. Gubin

*Institute of Solar-Terrestrial Physics SB RAS,
Irkutsk, Russia, gubin@iszf.irk.ru*

A.A. Kochanov

*Institute of Solar-Terrestrial Physics SB RAS,
Irkutsk, Russia, kochanov@iszf.irk.ru*

V.V. Grechnev

*Institute of Solar-Terrestrial Physics SB RAS,
Irkutsk, Russia, grechnev@iszf.irk.ru*

E.F. Ivanov

*Institute of Solar-Terrestrial Physics SB RAS,
Irkutsk, Russia, eugenessrt@gmail.com*

V.S. Kobets

*Institute of Solar-Terrestrial Physics SB RAS,
Irkutsk, Russia, kobets@iszf.irk.ru*

N.S. Meshalkina

*Institute of Solar-Terrestrial Physics SB RAS,
Irkutsk, Russia, nata@iszf.irk.ru*

A.A. Muratov

*Institute of Solar-Terrestrial Physics SB RAS,
Irkutsk, Russia, mutolya@mail.ru*

D.V. Prosovetsky

*Institute of Solar-Terrestrial Physics SB RAS,
Irkutsk, Russia, proso@iszf.irk.ru*

I.I. Myshyakov

*Institute of Solar-Terrestrial Physics SB RAS,
Irkutsk, Russia, ivan_m@iszf.irk.ru*

A.M. Uralov

*Institute of Solar-Terrestrial Physics SB RAS,
Irkutsk, Russia, uralov@iszf.irk.ru*

A.Yu. Fedotova

*Institute of Solar-Terrestrial Physics SB RAS,
Irkutsk, Russia, fedotovanstya@iszf.irk.ru*

Abstract. The article discusses characteristics, fundamental and applied tasks of the Siberian Radioheliograph that is developed at the ISTP SB RAS Radio Astrophysical Observatory and spectropolarimetric complex that measures the total flux of solar radio emission. The multiwave mapping of the Sun in the microwave range is a powerful and relatively inexpensive, in comparison with space technologies, means of observing solar activity processes and diagnosing plasma parameters. All-weather monitoring of electromagnetic solar emission (in the range from meter to millimeter waves, including measurements of the solar activity index at 2.8 GHz), and at the location of other diverse diagnostic

facilities of the Heliogeophysical Complex, is of particular value. Radioheliograph data is necessary to develop and implement methods of short-term forecast of solar flares, measurements of kinematics and characteristics of coronal mass ejection plasma, forecast of characteristics of fast solar wind streams.

Keywords: radioheliograph, Sun, magnetic fields, monitoring, particle acceleration.

INTRODUCTION

Solar electromagnetic emission and plasma streams are dominant external factors that determine the variability of properties of near-Earth space, which is actively explored using state-of-the-art technologies. The main impacts on near-Earth space are associated with recurrent structures in the solar wind (fast solar wind streams from coronal holes, corotation regions of fast and slow streams), ionizing emission, hard radiation from solar flares, radio bursts, coronal mass ejections (CMEs), and solar energetic particles. The geoeffective impacts lead to geomagnetic storms, ionospheric disturbances, and atmosphere heating, which in turn cause various practical consequences: currents in pipelines and electrical networks, failures in civil and military communication and navigation systems, electrostatic charging of spacecraft surfaces, increased atmospheric drag, etc.

Research into energy release processes in the solar atmosphere — both gradual ones resulting in heating of the chromosphere and corona and sporadic ones manifesting themselves in solar flares and CMEs — consumes considerable material and intellectual resources. Continuous monitoring of solar activity in 1–8 Å soft X-ray has been performed by NASA with GOES satellites since 1977. The Sun is observed with spacecraft such as SOHO [Domingo et al., 1995], STEREO-A [Kaiser et al., 2008], Hinode [Kosugi et al., 2007], SDO [Pesnell et al., 2012], IRIS [de Pontieu et al., 2014], and Parker Solar Probe [Fox et al., 2016]. Space-borne observations are supplemented by data from the global network of large ground-based solar-dedicated instruments.

In a radio frequency band, the continuous monitoring of solar activity is carried out by the Radio Solar Telescope Network (RSTN) [Kennewell, 1998] and e-Callisto

[Benz et al., 2009]. Radio observations are important and in some problems represent a unique source of information about solar activity processes. On the one hand, they allow us to monitor and diagnose the current state of solar activity in a wide range of time scales and in a very large dynamic range of variations in emission fluxes. On the other hand, the solar radio emission provides information about the nature of sources of effective emissions, which is necessary to develop a theory of impulsive energy release on the Sun and algorithms of its forecast.

Let us consider the basic factors of solar activity. CMEs are closely related to solar flares and are initiated by destabilization of magnetic flux ropes in the lower corona and their ejection into the outer corona. The velocity of the ejected plasma can exceed 3000 km/s, and the kinetic energy of the ejections is comparable with the energy of powerful flares. CMEs can cause the severest disturbances of Earth's magnetoplasma sheaths and can lead to the appearance of solar cosmic rays, accelerated by shock waves propagating ahead of them. Radio observations make it possible to monitor CMEs against the background of the solar disk, from the beginning of magnetic flux rope rise during its acceleration. It is important that in radio emission we can detect both populations of ejected plasma — thermal and accelerated. One of the fundamental problems of understanding the nature of flares and CMEs is to elucidate the contributions of processes in the flare region in the lower corona and shock waves, formed at the fronts of CMEs on their way to Earth, to the acceleration of solar energetic particles [Zhang et al., 2007; Grechnev et al., 2008, 2018; Chertok et al., 2015].

The most dynamic processes responsible for near-Earth space disturbances occur in the solar corona. Solar flares produce hard electromagnetic emission and accelerated particles that deteriorate radiation conditions in near-Earth space and pose hazard for spacecraft equipment and crew members. Intense electromagnetic emission and high-energy particles can directly affect the ionosphere [Afraimovich et al., 2001, Tsurutani et al., 2009, Yasyukevich et al., 2018]. Radio emission of flares comprises two main components. The first of them, mainly below 3 GHz, is generated by electrons with energies of tens and hundreds of kiloelectronvolt through coherent mechanisms, and the second component is emitted by electrons with energies up to several megaelectronvolt through the incoherent gyrosynchrotron mechanism.

Of particular note are powerful solar bursts generated by coherent mechanisms in active regions, shock waves, and flares. The intensity of their emission can be as high as 10^{-16} W/(m²·Hz) in the earth's surface and lead to disruptions of communication and navigation systems, flashes on civil and military radars [Bala et al., 2002; Knipp et al., 2016; Marqué et al., 2018]. In particular, there were events in which the emission intensity at 2800 MHz (*F*_{10.7} index) increased by two orders of magnitude relative to the quiet-Sun level [Cerruti et al., 2006]. Particularly noteworthy in this regard is the generation of powerful narrowband bursts, so-called

spikes, in the corona [Fleishman, Melnikov, 1998; Chernov, 2006; Treumann, 2006], characterized by a sudden increase in emission by several orders of magnitude in a narrow band.

Electromagnetic emission of a powerful solar flare in ultraviolet and X-rays reaches the vicinity of Earth within eight minutes and causes sudden ionospheric disturbances and radio blackouts lasting from a few minutes to several hours. The radio interference can last for more than ten hours. Proton precipitation in polar regions is accompanied by absorption of radio waves in the polar cap and communication failures for a few days. These factors are precursors of a magnetospheric storm.

A significant contribution to disturbances in near-Earth space can be made by fast wind streams from coronal holes in the solar atmosphere and processes in regions of their interaction with slow wind streams. Microwave radio observations allow us to identify coronal holes on the solar disk and forecast characteristics of generated fluxes [Krieger et al., 1973; Tsurutani et al., 2006].

When studying energy release on the quiet Sun, a topical problem is that of corona heating and especially of identifying sources of emission with a wavelength of 10.7 cm — a key index of solar activity [Schonfeld et al., 2015].

The most important among the fundamental problems of solar physics is the magnetography of coronal structures. Currently there is no doubt that an energy source for dynamic processes in the solar corona is the magnetic field. Variations in photospheric fields generate currents in the corona and form unstable magnetic structures. Fast relaxation of their nonpotential energy shows up as an impulsive energy release. Early identification of such configurations and monitoring of their evolution will allow us to predict the time of initiation of eruptive events and their power.

It should be noted that magnetic field strength and direction significantly affect microwave emission characteristics. We can therefore observe anomalies in distributions of microwave sources in flare-productive active regions, which are caused by changes in the plasma density and magnetic field during storage of nonpotential energy of magnetic fields, before powerful geoeffective flares. Differences between distributions of microwave sources in flare-productive active regions and typical configurations in quiet regions allowed researchers [Tanaka, Enome, 1975; Maksimov et al., 1996; Smolkov et al., 2010] to develop a statistically sound algorithm for short-term forecast of powerful flares. The elaboration of this method has demonstrated that the forecast success rate increases if multi-frequency images of an evolving active region are analyzed [Smolkov et al., 2009]. The method relies on relatively simple morphological relationships and can be algorithmized [Maksimov, Prosovetsky, 2005].

Uralov et al. [2006, 2008] have shown that the appearance of quasi-stationary sources above the inversion line of the radial magnetic component on radio maps produced by SSRT and Nobeyama Radioheliograph (NoRH [Nakajima et al., 1994]) indicates the

possibility of powerful flares in their vicinity. The appearance of such sources is attributed to the emergence of a new magnetic flux to the atmosphere of the active region and to the formation of a current sheet — their connection with energy release sites in the corona has been confirmed experimentally.

Indications of the possibility of detecting current structures from data on the spectrum of active region microwave emission have been found in [Tokhchukova, Bogod, 2003]. Using these detailed observations of the emission spectrum of active regions, obtained by the multifrequency receiver of RATAN-600, the authors have identified a number of new effects which can be employed to develop algorithms for forecasting flare productivity from radio data. In particular, if the polarization sign changes twice in a relatively narrow band of the emission spectrum of a flare-productive active region, a flare is expected [Kaltman et al., 2005]. At RATAN-600, methods for short-term forecast of powerful flares from features of structure and dynamics of microwave sources are also being developed [Abramov-Maksimov et al., 2014].

In recent decades, it was established that CMEs transfer so-called magnetic clouds to Earth, in which the magnetic field direction drastically affects geoeffectiveness of solar wind disturbances. The problem of determining the structure of magnetic fields in the CME source region is, therefore, crucial not only for the eruption forecast, but also for the assessment of the level of subsequent geomagnetic disturbances, i.e. for the development of scientific bases for methods of geomagnetic activity forecast [Grechnev et al., 2014].

Optical methods cannot be used to measure coronal magnetic fields because for this purpose it is necessary to isolate magnetoactive emission lines of the optically thin corona against the bright solar disk [Stenflo, 2010]. New-generation solar infrared telescopes will use infrared coronal lines, but in this case measurements will be effective only over the solar limb [Tritschler et al., 2016]. Nowadays, eruptive events are interpreted using methods for calculating magnetic fields in potential and nonlinear force-free approximations. As observed boundary conditions the magnetograms obtained in optically thick photospheric layers are utilized (see, e.g., [Rudenko, Myshyakov, 2009]). This approach provides only a first approximation since it ignores current sheets — key elements of flare energy release — and does not consider the evolution of magnetic configuration.

Magnetic fields in the corona can be measured from characteristics of solar radio emission since the contribution of the coronal emission in this range is significant as compared to photospheric and chromospheric emissions [Akhmedov et al., 1982]. Radio magnetography methods are based on the well-developed theory of bremsstrahlung and gyroresonance emission mechanisms and on the circular polarization reversal effects when the emission propagates through regions with so-called quasi-transverse magnetic fields.

It is necessary to bear in mind that the measured radio spectra include the contribution of emission layers along the line of sight with different optical thickness. The correct interpretation of observations of coronal structures therefore requires a three-dimensional model of sources consistent with all available observational data in different spectral ranges — not only in the radio range, but also in X-rays and in the extreme ultraviolet..

Efficiency of routine diagnostics of magnetic fields of active regions with the aid of multiwave microwave observations has been demonstrated in studies based on RATAN-600 observations (see [Kaltman et al., 2005; Kaltman et al., 2013, 2015] and references therein), using a 112-channel receiving spectral complex with an operating frequency band from 0.756 to 18.2 GHz. Unfortunately, the RATAN-600 knife-edge beam pattern restricts the capabilities of the coronal magnetography, based on data from this instrument.

To date, the diagnostic potential of radio methods is hampered by lack of adequate instrumentation. Modern radio astronomical observations of the Sun should be based on data from multiwave radioheliographs, which can measure radio emission spectra with a spatial resolution sufficient to identify the main coronal elements of active regions in solar images, i.e. magnetic loops as small as several arcseconds. The temporal resolution should ensure the detection of individual events of flare energy release that can be as short as 1 s. Observations with radioheliographs should be supplemented by data from spectropolarimeters of the total solar emission, which are used to extend the frequency range of observations at high spectral resolution.

Advances in electronic and computer technologies of the last decade have opened up opportunities to construct radio telescopes with necessary characteristics. The concept of the Frequency Agile Solar Radiotelescope (FASR) with record parameters in spatial, temporal, and frequency resolution proposed by U.S. scientists in 1999 [Gary et al., 2001] has encouraged Chinese (Mingantu Spectral Radioheliograph, MUSER [Yan et al., 2009]) and Russian scientists (Siberian Radioheliograph, SRH [Lesovoi et al., 2012]) to develop similar projects, which are now at various stages of implementation. In U.S., the FASR concept is used to gradually supplement the Expanded Owens Valley Solar Array (EOVSA, [Gary et al., 2018a]).

Also noteworthy are some modern radio telescopes that are occasionally used to address problems of solar physics: Very Large Array (VLA, USA), LOw Frequency ARray (LOFAR), Atacama Large Millimeter Array (ALMA). First multi-frequency data is available now from two new instruments at two-dimensional resolution — SRH prototype [Lesovoi et al., 2017] and EOVSA [Gary et al., 2018b]. We can expect an unprecedented increase in the use of the microwave diagnostics of active regions and solar flares, which will lead to a qualitatively new understanding of the nature of solar activity processes.

In this paper, we discuss the Siberian Radioheliograph developed at ISTP SB RAS.

1. SIBERIAN RADIOHELIOGRAPH

The Siberian Radioheliograph (SRH) is developed according to RF Government Decree No. 522 of April 28, 2018 at the ISTP SB RAS Radio Astrophysical Observatory, which allows us to make observations with SRH in combination with the existing instruments and to use the observatory infrastructure (available housing, communications, transport). The observatory is at 220 km from Irkutsk ($51^{\circ}45'33''$ N, $102^{\circ}13'08''$ E). The choice of the site is determined, above all, by the existing infrastructure of the Radio Astrophysical Observatory and low level of RF interference due to its isolated location from major population centers.

The SRH concept and objective have been developed under the leadership of A.T. Altyntsev and S.V. Lesovoi at the ISTP SB RAS Radio Astrophysical Department. Researchers of the department have extensive experience of operating and upgrading the Siberian Solar Radio Telescope (SSRT) with the 256-antenna array with a baseline of 622 m [Smolkov et al., 1986; Grechnev et al., 2003]. SSRT radio maps at a frequency of 5.7 GHz were used in many Russian and international projects on the study of signs of flare productivity of active regions and mechanisms of coronal heating in coronal holes, where high-speed solar wind streams are formed, etc. SSRT has provided new knowledge about the nature and kinematics of CME, mechanisms of primary energy release and particle acceleration in solar flares.

In developing the concept, we have formulated the following topical scientific problems that will be solved with the aid of SRH:

- configurations and strengths of coronal magnetic fields in active regions, flare loops, CMEs, and the quiet Sun's atmosphere;
- diagnostics of magnetoplasma characteristics and accelerated particles in regions of energy release;
- identification of electron acceleration mechanisms, flare plasma heating, and energy transport and transformations in the solar atmosphere;
- detection and investigation of wave processes and shock waves in the solar atmosphere;
- study of the evolution of large-scale structures in the solar atmosphere with time scales of the order of the solar cycle;
- development of methods for indexing solar activity based on characteristics of radio emission;
- development of new instruments for monitoring solar activity in radio frequency band.

The full use of the potential of radio observations requires a comprehensive research methodology relying on the most modern tools of 3D modeling, which requires observational data from other observation ranges (X-ray, ultraviolet, etc.), correct methods for reconstructing the coronal magnetic field, tried and tested models of chromosphere and corona heating, optimized methods for rapid calculation of parameters of electromagnetic emission.

The applied problems that will be addressed using

data from SRH and accompanying spectropolarimeters of total solar emission:

- measurements of the total flux of radio emission at 10.7 cm, which is a conventional solar activity index;
- short-term forecast of powerful solar flares in advance of two to three days;
- monitoring of solar radio emission in a wide range, including operating frequencies of different ground-based instruments such as radars, navigation and communication systems;
- diagnostics of geoeffective parameters of solar flares;
- providing original data for Russian and international centers for solar activity monitoring.

1.1. Technical characteristics of SRH

SRH is an interferometer designed to produce solar images in the 3–24 GHz frequency range in both circularly-polarized components. The field of view of the radioheliograph should exceed the size of the solar disk, thus restricting the diameter of individual antennas. The interferometer consists therefore of three separate antenna arrays for 3–6, 6–12, 12–24 GHz frequency bands (Figure 1) with antenna diameters of 3, 1.8, and 1 m respectively. The numbers of antennas in the arrays are 129, 192, 207. T-shaped antenna arrays for 3–6 and 6–12 GHz frequency ranges are equidistant, and in the 12–24 GHz antenna array the spacing between outer antennas is increased relative to the central antennas. The altazimuth antenna mounting will ensure the observable object tracking accuracy not lower than 5 arcmin.

The choice of redundant T-shaped arrays is determined by i) the possibility of using the redundancy in calibrations of the antenna gains in such arrays, and ii) the high sensitivity required for spectral polarization measurements the radioheliograph would perform. In determining the maximum interferometer base, we took into account that the spatial resolution of microwave solar observations is limited by emission scattering by small-scale plasma fluctuations in the corona [Bastian, 1994; Altyntsev et al., 1996; Chashei et al., 2006]. According to these works, the apparent size of a point-like solar source at ~6 GHz is at least 5 arcsec.

Maps with a higher spatial resolution will be available in studying bright flare sources with the Chinese MUSER radioheliograph with a 0.4–15 GHz operating



Figure 1. Schematic arrangement of antenna arrays of the Siberian Radioheliograph

frequency range, which is currently under construction in Inner Mongolia [Yan et al., 2009]. When studying bright flare sources, high-sensitivity SRH observations at higher frequencies would be supplemented by Chinese data of a higher spatial resolution (see Table 1).

Fiber-optic links are used to transmit antenna signals to the working building. Each link has an optical modulator, an optical fiber, and an optical demodulator.

Receiving systems of the arrays are independent and consist of analog and digital blocks. The analog block converts optical signals from antennas into microwave signals, amplifies them and downconverts to the first

intermediate frequency. Functions of the digital block of the receiving system are to convert the signal into digital form, to form the operating frequency band, to compensate a geometric delay, to perform fringe stopping, and to form quadrature signals *I* and *Q*. Digital receivers are controlled via a local computer network.

Data acquisition and storage software controls the observational mode of the radioheliograph according to the schedule specified in configuration files; provides the graphics user interface to monitor the state of the SRH systems and the observational modes;

Table 1

SRH main parameters

Frequency band, GHz	Spatial resolution, arcsec	Temporal resolution in single-frequency imaging mode	Spectral resolution, MHz	Dynamic range for the input signal power, dB	Dynamic range of images, dB	Flux-density sensitivity (accumulation time of 0.1 s in single-frequency imaging mode), $W/(m^2 \cdot Hz)$
3–6	15–30	accumulation time up to 0.1 s	10	30	23	$40 \cdot 10^{-26}$
6–12	12–24				23	$70 \cdot 10^{-26}$
12–24	7–13				20	$250 \cdot 10^{-26}$

provide visualization of the data and its storage in the FITS format. The control of the observational mode involves managing the list of operating frequencies. To observe fast processes, a small number of frequencies with 1-s imaging interval are chosen. To measure quasi-stationary structures such as active regions with a high spectral resolution, a longer (e.g. 1-minute) imaging interval is set.

The antenna arrays will be put into regular operation by stages. In 2020, we plan to start observations in the 3–6 GHz band, then to put into operation the 12–24 GHz array, and finally the 6–12 GHz array.

1.2. Total flux spectropolarimeters

Multiwave SRH observations would be supplemented by total flux spectra of polarized solar emission in the range from short centimeter to meter wavelengths.

The *S-band spectropolarimeter* measures the intensity *I* and circular polarization *V*. The whole observing frequency range will be divided into two bands served by antennas of different diameters (Table 2).

Table 2

Antenna diameters, m	1 and 3
Frequency band, GHz	3–24
Frequency resolution, MHz	10
Dynamic range, dB	60
Temporal resolution, s	0.1

This spectropolarimeter is designed to monitor solar emission with a high spectral and temporal resolution in a wide frequency range sufficient to detect narrowband spikes. Spectropolarimeter data will also be used for calibration of SRH data, especially during strong microwave bursts.

The main purpose of the VHF–UHF spectropolarimeter is to monitor CME emission and RF interference level in the frequency bands of GPS, GLONASS, Beidou, and Galileo navigation satellite networks (1100–1610 MHz). In the VHF band, a log-periodic antenna with perpendicular vibrators and aligned centers is employed.

Total-flux measurements, e.g. at 2.8 GHz, can be used as solar activity indices (Table 3).

Table 3

Frequency band, MHz	50–3000
Dynamic range, dB	40
Temporal resolution, s	0.1
The number of frequency channels	500

1.3. Technological groundwork and tests of radioheliograph systems

The multiwave radioheliograph would not be designed without multi-year engineering development carried out by the ISTP SB RAS team. Technical solutions and devices of the multiwave radioheliograph were tested in situ, using interferometer prototypes in a frequency band of 4 to 8 GHz whose antennas were installed on SSRT mounts. The first prototype consisting of ten antennas located at outer SSRT posts with a maximum baseline of 622.3 m started working in 2010 [Lesovoi et al., 2012]. We tested solutions for designing systems of data collection in fiber lines, broadband feed elements, local oscillators, analog and digital receivers, correlator. This prototype was used for regular solar observations and provided new results. In particular, the experiments showed a significant effect of variations in size of sources with frequency on the form of integrated microwave spectra of flares [Altyntsev et al., 2012].

The next stage was the 48-antenna radioheliograph, which commenced observations in 2016. Its design and first results are presented in [Lesovoi et al., 2017; Lesovoi, Kobets, 2018; Lesovoi et al., 2014; Grechnev et al., 2018; Fedotova et al., 2018]. SRH-48 was developed under the Federal Target Program "Development and elaboration of a system to monitor geophysical conditions over the territory of the Russian Federation for 2008–2015". Antennas of SRH-48 are installed on SSRT mounts near the center of the array with a longest baseline of 107.4 m (Figure 2). Besides elaborating technical issues, the development of SRH-48 allowed us to start designing software for image reconstruction and methods of their calibration. SRH-48 has started regular monitoring of solar activity with online presentation of observational data on the Internet (Figure 3). The test results and the first scientific results obtained using the prototypes have confirmed the validity of the chosen solutions and have assured that parameters of this instrument will correspond to the desired ones.



Figure 2. Part of the antenna array SRH-48. Antenna diameter is 1.8 m; distance between antennas is 4.9 m. The larger remote white antennas belong to the SSRT array. Signals from the SRH antennas are transmitted via fiber links in the tunnel to the working building visible behind the antennas

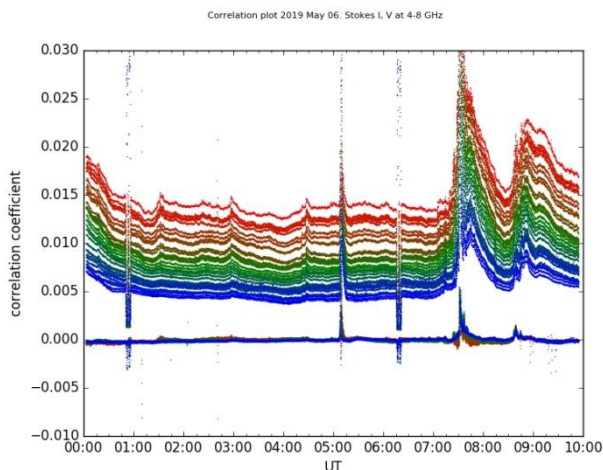


Figure 3. Correlation curves of SRH-48 recorded at 32 frequencies at 4–8 GHz on May 06, 2019. Upper curves show intensity variations (frequencies increasing from top to bottom); lower curves, circular polarization variations. Responses to M1.0 (05:10), C1.7 (07:23), C2.0 (08:41) flares and intervals of amplitude calibrations at 00:45 and 06:20 are shown. Time refers to UTC

The operation of the radioheliograph and solar activity are monitored using the correlation curves that represent the sum of cross-correlation functions of signals from all antenna pairs [Lesovoi, Kobets, 2017]. The cross-correlation is roughly proportional to the solar flux at a given frequency. The correlation curves in Figure 3 obtained at 32 frequencies on May 6, 2019 demonstrate that a ground-based instrument can detect solar flares as weak as GOES C class or even lower. Correlation curves and solar images produced by SRH-48 at all operating frequencies are posted in real time on the web page [<http://badary.iszf.irk.ru/sr-CorrPlot.php>]. In particular, the sets of images allow one to locate an eruptive event on the Sun, which is important to assess its expected space-weather impact.

Figure 4 exemplifies the observation of an eruptive filament. Despite the low spatial resolution of SRH-48, it provides images that reproduce the shape of the eruptive filament, which was also observed by the Japanese Nobeyama Radioheliograph at a higher frequency and by the ultraviolet telescope AIA on board NASA's Solar Dynamics Observatory (SDO). SRH-48 observations of plasma ejections are presented in [Fedotova et al., 2018; Grechnev et al., 2018]. After completion of the SRH construction, its beam size at 6 GHz will be close to that of the Nobeyama Radioheliograph shown in Figure 4. The SRH spatial resolution will be high enough to discern the structure of ejections, while estimates of their plasma density and temperature distributions can be obtained from SRH spectra.

1.4. Measurements of total flux spectra

Total flux spectropolarimeters readily detect solar flares and evaluate their intensity. The appearance of weak radio bursts is one of the most important predictors of powerful flares. Important characteristics of the spectropolarimetric observations are their all-weather performance capability and relative cheapness as compared to satellite observations. The round-the-clock total flux measured by RSTN [Kennewell, 1998] at frequencies of 245, 410, 610, 1415, 2695, 4995, 8800, 15400 MHz with a time resolution of 1 s is available on the Website [<https://www.ngdc.noaa.gov>]. Total flux measurements at the Nobeyama Observatory [Torii et al., 1979; Nakajima et al., 1985] in intensity and circular polarization at 1, 2, 3.75, 9.4, 17, and 35 GHz and only in intensity at 80 GHz with a routine time resolution of 1 s and 0.1 s during strong bursts are available on the Website [<https://solar.nro.nao.ac.jp/norp>]. In both cases, the data is not available in real time. In the VLF range (generally 45–870 MHz), the global network e-CALLISTO is deployed to monitor CMEs [Benz et al., 2009].

At the Radio Astrophysical Observatory, SRH-48 observations are accompanied by spectropolarimeters with operating frequency bands 2–24 GHz (16 channels, 1.6 s temporal interval) and 4–8 GHz (26 channels, 10 ms) [Muratov, 2011; Zhdanov, Zandanov, 2015].

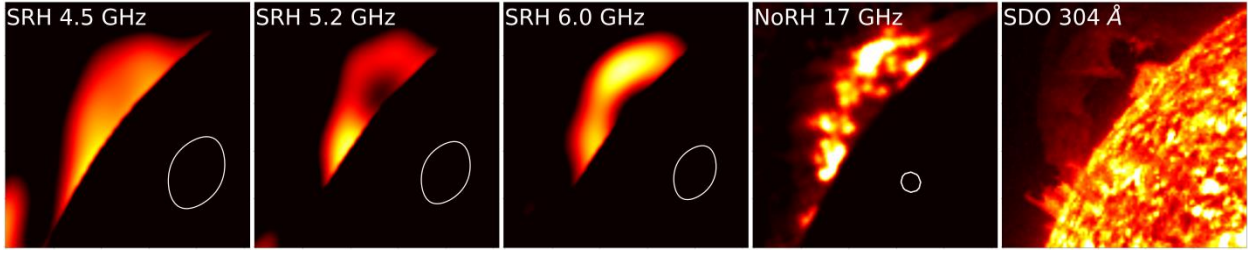


Figure 4. Rise of a filament over the solar limb on April 24, 2017 (03:10 UT). Panels 1–3 present images taken with SRH-48 at 4.5–6.0 GHz, Nobeyama at 17 GHz, and SDO/AIA at a wavelength of 304 Å. Frame size is 400×400 arcsec. Ovals indicate beams of interferometers at corresponding frequencies

The spectropolarimeters, whose characteristics are listed in Section 1.2, will be constructed using modern hardware components. Their data will provide solar activity indices for models of the magnetosphere and ionosphere. Besides the well-known F10.7 index, of practical interest is, for example, F30, which is better correlated with atmospheric drag of satellites in low orbits (< 1000 km) [Yaya et al., 2017].

1.5. Data analysis techniques

The effective use of SRH data requires algorithms for the analysis of large solar image sequences at dozens of frequencies in the 3–24 GHz range. To ensure a widespread use of the data, the website will present correlation curves and solar images at selected frequencies in real time. The basic techniques have been tried and tested using SRH-48 data. In Figure 5 is the web page [http://badary.iszf.irk.ru/srhCorrPlot.php] with correlation curves obtained at 32 frequencies in the 4–8 GHz range in intensity (R+L) and circular polarization (R–L). On the right are raw images at the moment of observation. The web page is updated every few minutes.

To provide remote access to SRH observations, data archives, catalogs, and software packages will be developed in Python to synthesize and deconvolve images and

to calculate spectral characteristics of the structures of interest in the intervals specified. In studies that will use data from multiwave radioheliographs, employment is intended for 3D modeling tools, which will implement methods of reconstructing magnetic field in the corona, approved models of chromospheric and coronal heating, and optimized methods for quick calculation of electromagnetic emission spectra in intensity and polarization.

Interactive methods for modeling radio spectrum from solar images are developed considering dominant radio emission mechanisms, i.e. gyroresonance, gyro-synchrotron, and bremsstrahlung [Fleishman et al., 2019; Gary et al., 2019]. Parameters of thermal plasma and accelerated electrons are set to make model emission distributions in radio, ultraviolet, and X-rays close to available observations. The model parameters are found by achieving the best fit between the 3D model and observed 2D radio maps at different frequencies. By repeating this procedure, it will be possible to obtain evolving distributions of parameters of magnetic field and accelerated electrons in flare loops. This will for the first time enable us to examine the evolution of the magnetic field in flares, magnetic energy storage and relaxation, initiation of eruptive events.

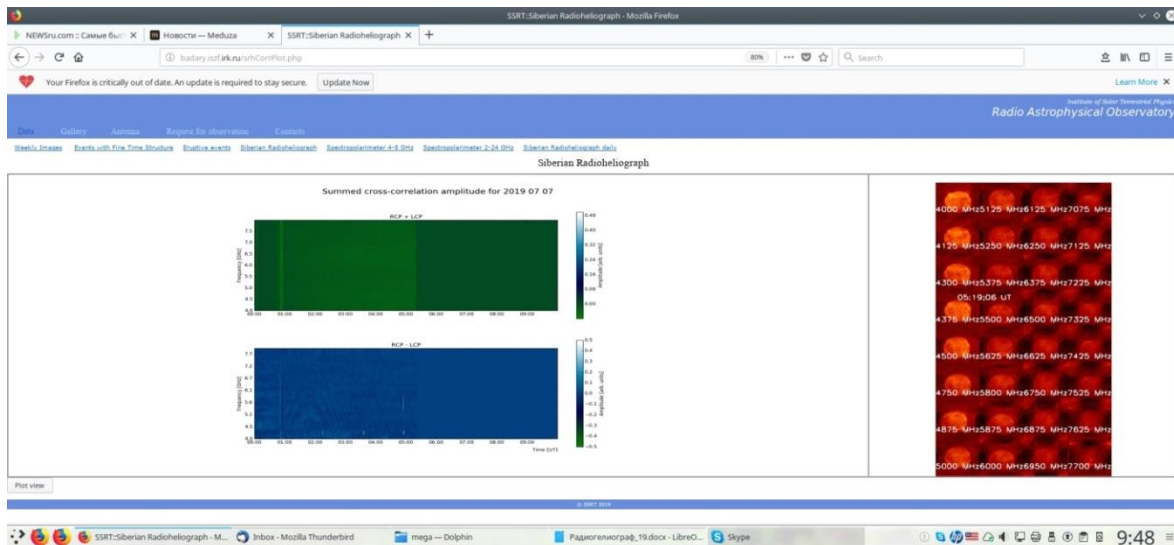


Figure 5. Website [http://badary.iszf.irk.ru/srhCorrPlot.php] during observation on July 7, 2019. Correlation dependences at 32 frequencies in the 4–8 GHz range in intensity (R+L) and circular polarization (R–L). On the right are raw images at the time of observation

Technologies for 3D modeling of dynamic coronal structures in the solar atmosphere, based on microwave data, are developed by ISTP SB RAS, a number of Russian institutes (SAO RAS, Ioffe Institute, St. Petersburg State University), and by the solar team at the New Jersey Institute of Technology [Fleishman et al., 2019; Gary et al., 2019; Kuznetsov, Kontar, 2015]. The use of the models will allow us to radically improve the forecast and diagnostics of geoeffective eruptive events such as solar flares and CMEs [Fleishman, Kuznetsov, 2010; Wang et al., 2015; Fleishman et al., 2018].

The next important field for the use of SRH data is the study of energy release processes in the solar atmosphere, both gradual, which are responsible for chromospheric and coronal heating, and sporadic, which are manifested in flares and CMEs. Radio observations supplement measurements in hard X-rays with data on accelerated particles, being sensitive to structures, whose low plasma density is typical of the corona. SRH data is promising in addressing the following problems: triggers of flares and CMEs, mechanisms of heating and particle acceleration in flares, CME acceleration, magnetic reconnection rates and characteristic scales of elementary acts of energy release, plasma parameters in coronal holes, where the high-speed solar wind originates.

Due to the uniformity and wide dynamic range, data provided by radioheliographs is promising for studies of the patterns that govern power, spatial and temporal distributions of energy release processes. In particular, the analysis of scattering of microwave emission in the lower corona has revealed the flicker character of the power spectra of turbulent plasma density perturbations in regions, where solar wind streams were formed [Chashei et al., 2006]. Of considerable interest is data on the evolution of large-scale magnetic structures on time scales exceeding the solar cycle [Shibasaki, 2013]. The study of self-organization of solar phenomena is crucial for the determination of the lead time of their reliable forecast. Figure 6 shows a synoptic radio brightness distribution obtained from SSRT daily full-disk intensity images at 5.7 GHz. The so-called Maunder butterflies show up which reflect the progressive drift toward the equator of active regions during solar cycle 23.

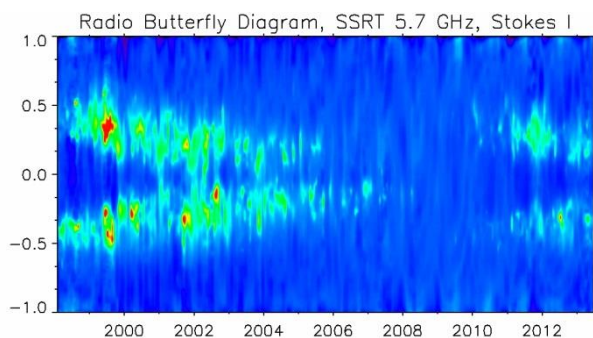


Figure 6. Synoptic diagram of microwave emission intensity in solar cycle 23 at 5.7 GHz from SSRT data

CONCLUSION

Multi-frequency imaging of the Sun in microwaves is a powerful and relatively inexpensive means to monitor solar activity processes and diagnose plasma parameters as compared to space technologies. Radio observations become especially important in the next decade when possibilities of space-borne spectral observations in hard X-rays and gamma-rays would be limited.

The main problems addressed using multiwave radioheliographs are the formation of unstable coronal magnetic configurations and their impulsive relaxation, identification of acceleration mechanisms (quasi-static electric fields, stochastic acceleration, and shock waves), evaluation of the contributions of energy and particle transfer effects (trapping of particles in magnetic structures, scattering and acceleration of particles in interactions with turbulence, heating of coronal and chromospheric regions of the solar atmosphere).

A large number of governmental institutions and commercial firms in Russia are interested in accurate prompt reports on heliogeophysical and space weather conditions. The absence of a domestic space-borne and ground-based complex for continuous monitoring of solar activity complicates the situation. This fact determines the dependence of Russia on foreign (mainly U.S. and EU) systems that monitor the processes on the Sun and in near-Earth space. In this respect, the all-weather monitoring of electromagnetic solar emission (from meter to millimeter wave bands, including measurements of the solar activity index at 2.8 GHz) at the location of various diagnostic instruments of the Heliogeophysical complex is of particular value. Methods for short-term forecast of solar flares, measurements of CME kinematical characteristics and parameters of their plasma, forecast of characteristics of fast solar wind streams will be developed.

Development and construction of a complex of new large experimental facilities with advanced capabilities will allow world-class research in this field and establish strategic groundwork for 20–30 years. Implementation of breakthrough projects relying on the unique observational data will attract leading and young specialists from Russia and abroad.

The work was performed with budgetary funding of Basic Research program II.16.3.2. "Nonstationary and wave processes in the solar atmosphere", the project "Primary energy release and turbulence in solar flares" under RAS Presidium Basic Research program KP 19-270 "Space: research into fundamental processes and their relationships", and supported by the Russian Science Foundation under grant 18-12-00172.

The experimental data were obtained using the Unique Research Facility Siberian Solar Radio Telescope [<http://ckp-rf.ru/usu/73606>].

REFERENCES

Abramov-Maksimov V.E., Borovik V.N., Opeikina L.V., Tlatov A.G. Peculiarities in evolution of solar active regions before powerful X class flares: analysis of RATAN-600 and SDO space observatory data. *Kosmicheskie issledovaniya*

[Cosmic Res.]. 2014, vol. 52, iss. 1, p. 3. DOI: [10.7868/S0023420614010014](https://doi.org/10.7868/S0023420614010014). (In Russian).

Afraimovich E.L., Altyntsev A.T., Kosogorov E.A., Larina N.S., Leonovich, L.A. Ionospheric effects of the solar flares of September 23, 1998 and July 29, 1999 as deduced from global GPS network data. *J. Atmos. Solar-Terr. Phys.* 2001, vol. 63, iss. 17, pp. 1841–1849. DOI: [10.1016/S1364-6826\(01\)00060-8](https://doi.org/10.1016/S1364-6826(01)00060-8).

Akhmedov Sh.B., Gelfreikh G.B., Bogod V.M., Korzhavin A.N. The measurement of magnetic fields in the solar atmosphere above sunspots using gyroresonance emission. *Solar Phys.* 1982, vol. 79, iss. 1, pp. 41–58. DOI: [10.1007/BF00146972](https://doi.org/10.1007/BF00146972).

Altyntsev A.T., Grechnev V.V., Kononov S.K., Lesovoi S.V., Lisyian, E.G., Treskov T.A., et al. On the apparent size of solar microwave spike sources. *Astrophys. J.* 1996, vol. 469, p. 976. DOI: [10.1086/177844](https://doi.org/10.1086/177844).

Altyntsev A.A., Fleishman G.D., Lesovoi S.V., Meshalkina N.S. Thermal to nonthermal energy partition at the early rise phase of solar flares. *Astrophys. J.* 2012, vol. 758, iss. 2, article id. 138, 12 p. DOI: [10.1088/0004-637X/758/2/138](https://doi.org/10.1088/0004-637X/758/2/138).

Bala B., Lanzerotti L.J., Gary D.E., Thomson D.J. Noise in wireless systems produced by solar radio bursts. *Radio Sci.* 2002, vol. 37, p. 1018. DOI: [10.1029/2001RS002481](https://doi.org/10.1029/2001RS002481).

Bastian T.S. Angular scattering of solar radio emission by coronal turbulence. *Astrophys. J.* 1994, vol. 426, no. 2, pp. 774–781. DOI: [10.1086/174114](https://doi.org/10.1086/174114).

Benz A.O., Monstein C., Meyer H., Manoharan, P.K., Ramesh R., Altyntsev A., et al. A world-wide net of solar radio spectrometers: e-Callisto. *Earth, Moon, and Planets.* 2009, vol. 104, iss. 1-4, pp. 277–285. DOI: [10.1007/s11038-008-9267-6](https://doi.org/10.1007/s11038-008-9267-6).

Cerruti A.P., Kintner P.M., Gary D.E., Lanzerotti L.J., de Paula E.R., Vo H.B., et al. Observed solar radio burst effects on GPS/wide area augmentation system carrier-to-noise ratio. *Space Weather.* 2006, vol. 4, iss. 10, CiteID S10006. DOI: [10.1029/2006SW000254](https://doi.org/10.1029/2006SW000254).

Chashei I.V., Shishov V.I., Altyntsev A.T. Apparent angular sizes of the sources of microwave subsecond pulses and electron-density fluctuations in the lower solar corona. *Astron. Rep.* 2006, vol. 50, iss. 3, pp. 249–254. DOI: [10.1134/S1063772906030085](https://doi.org/10.1134/S1063772906030085).

Chernov G.P. Solar radio bursts with drifting stripes in emission and absorption. *Space Sci. Rev.* 2006, vol. 127, iss. 1-4, pp. 195–326. DOI: [10.1007/s11214-006-9141-7](https://doi.org/10.1007/s11214-006-9141-7).

Chertok I.M., Abunina M.A., Abunin A.A., Belov A.V., Grechnev V.V. Relationship between the magnetic flux of solar eruptions and the A_p index of geomagnetic storms. *Solar Phys.* 2015, vol. 290, iss. 2, pp. 627–633. DOI: [10.1007/s11207-014-0618-3](https://doi.org/10.1007/s11207-014-0618-3).

Domingo V., Fleck B., Poland A.I. The SOHO mission: An overview. *Solar Phys.* 1995, vol. 162, iss. 1-2, pp. 1–37. DOI: [10.1007/BF00733425](https://doi.org/10.1007/BF00733425).

de Pontieu B., Title A.M., Lemen J.R., Kushner G.D., Akin D.J., Allard B., et al. The Interface Region Imaging Spectrograph (IRIS). *Solar Phys.* 2014, vol. 289, iss. 7, pp. 2733–2779. DOI: [10.1007/s11207-014-0485-y](https://doi.org/10.1007/s11207-014-0485-y).

Fedotova A.Yu., Altyntsev A.T., Kochanov A.A., Lesovoi S.V., Meshalkina N.S. Observation of eruptive events with the Siberian Radioheliograph. *Solar-Terr. Phys.* 2018, vol. 4, iss. 3, pp. 13–19. DOI: [10.12737/stp-43201802](https://doi.org/10.12737/stp-43201802).

Fleishman G.D., Melnikov V.F. Solar millisecond radio spikes. *Uspekhi fizicheskikh nauk* [Physics–Uspekhi (Advances in Physical Sciences)]. 1998, vol. 168, iss. 12, pp. 1265–1301. DOI: [10.3367/UFNr.0168.199812a.1265](https://doi.org/10.3367/UFNr.0168.199812a.1265). (In Russian).

Fleishman G.D., Kuznetsov A.A. Fast gyrosynchrotron codes. *Astrophys. J.* 2010, vol. 721, iss. 2, pp. 1127–1141. DOI: [10.1088/0004-637X/721/2/1127](https://doi.org/10.1088/0004-637X/721/2/1127).

Fleishman G.D., Nita G.M., Kuroda N., Jia S., Tong K., Wen R.R., Zhizhuo Z. Revealing the evolution of non-thermal electrons in solar flares using 3D modeling. *Astrophys. J.* 2018, vol. 859, iss. 1, article id. 17, 14 p. DOI: [10.3847/1538-4357/aabae9](https://doi.org/10.3847/1538-4357/aabae9).

Fleishman G., Bastian T.S., Chen Bin, Gary D.E., Glesener L., Nita G., et al. Solar coronal magnetic fields: quantitative measurements at radio wavelengths. Astro2020: Decadal Survey on Astronomy and Astrophysics, science white papers, no. 426. *Bull. American Astron. Soc.* 2019, vol. 51, iss. 3, id. 426.

Fox N.J., Velli M.C., Bale S.D., Decker R., Driesman A., Howard R.A., et al. The Solar Probe Plus Mission: Humanity's first visit to our star. *Space Sci. Rev.* 2016, vol. 204, iss. 1-4, pp. 7–48. DOI: [10.1007/s11214-015-0211-6](https://doi.org/10.1007/s11214-015-0211-6).

Gary D.E., Bastian T.S., White S.M., Hurford G.J. The Frequency-Agile Solar Radiotelescope (FASR). *Proc. Asia-Pacific Radio Science Conference AP-RASC '01*. Chuo University, Tokyo, Japan, 1–4 August, 2001, p. 236.

Gary D.E., Bastian T.S., Chen B., Fleishman G.D., Glesener L. Radio observations of solar flares. *Science with a Next Generation Very Large Array. ASP Conf. Ser.* 2018a, vol. 517, p. 99.

Gary D.E., Bin Chen, Dennis B.R., Fleishman G.D., Hurford G.J., Krucker S., et al. Microwave and hard X-ray observations of the 2017 September 10 solar limb flare. *Astrophys. J.* 2018b, vol. 863, iss. 1, article id. 83, 9 p. DOI: [10.3847/1538-4357/aad0ef](https://doi.org/10.3847/1538-4357/aad0ef).

Gary D., Bastian T.S., Chen Bin, Drake J.F., Fleishman G., Glesener L., et al. Particle acceleration and transport. New perspectives from radio, X-ray, and gamma-ray observations Astro2020: Decadal Survey on Astronomy and Astrophysics, science white papers, no. 371. *Bull. American Astron. Soc.* 2019, vol. 51, iss. 3, id. 371.

Grechnev V.V., Lesovoi S.V., Smolkov G.Ya., Krissinel B.B., Zandanov V.G., Altyntsev A.T., et al. The Siberian Solar Radio Telescope: the current state of the instrument, observations, and data. *Solar Phys.* 2003, vol. 216, iss. 1-2, pp. 239–272. DOI: [10.1023/A:1026153410061](https://doi.org/10.1023/A:1026153410061).

Grechnev V.V., Kurt V.G., Chertok I.M., Uralov A.M., Nakajima H., Altyntsev A.T., et al. An extreme solar event of 20 January 2005: Properties of the flare and the origin of energetic particles. *Solar Phys.* 2008, vol. 252, iss. 1, pp. 149–177. DOI: [10.1007/s11207-008-9245-1](https://doi.org/10.1007/s11207-008-9245-1).

Grechnev V.V., Uralov A.M., Chertok I.M., Belov A.V., Filippov B.P., Slemzin V.A., Jackson B.V. A challenging solar eruptive event of 18 November 2003 and the causes of the 20 November geomagnetic superstorm. IV. Unusual magnetic cloud and overall scenario. *Solar Phys.* 2014, vol. 289, iss. 12, pp. 4653–4673. DOI: [10.1007/s11207-014-0596-5](https://doi.org/10.1007/s11207-014-0596-5).

Grechnev V.V., Lesovoi S.V., Kochanov A.A., Uralov A.M., Altyntsev A.T., Gubin A.V., et al. Multi-instrument view on solar eruptive events observed with the Siberian Radioheliograph: From detection of small jets up to development of a shock wave and CME. *J. Atmos. Solar-Terr. Phys.* 2018, vol. 174, pp. 46–65. DOI: [10.1016/j.jastp.2018.04.014](https://doi.org/10.1016/j.jastp.2018.04.014).

Kaiser M.L., Kucera T.A., Davila J.M., St. Cyr O.C., Guhathakurta M., Christian E. The STEREO mission: An introduction. *Space Sci. Rev.* 2008, vol. 136, iss. 1-4, P. 5–16. DOI: [10.1007/s11214-007-9277-0](https://doi.org/10.1007/s11214-007-9277-0).

Kaltman T.I., Korzhavin A.N., Tsap Yu.T. On a change of sign of microwave emission polarization in solar spot radio sources. *Astronomicheskii zhurnal* [Astron. J.]. 2005, vol. 82, p. 838. (In Russian).

Kaltman T.I., Bogod V.M., Stupishin A.G., Yasnov L.V. Physical conditions in the low corona and chromosphere of solar active regions according to spectral radar measurements. *Geomagnetism and Aeronomy.* 2013, vol. 53, iss. 8, pp. 1030–1034. DOI: [10.1134/S0016793213080082](https://doi.org/10.1134/S0016793213080082).

- Kaltman T.I., Kochanov A.A., Myshyakov I.I., et al. Observations and modeling of the spatial distribution and microwave emission spectrum of the active region NOAA 11734. *Geomagnetism and Aeronomy*. 2015, vol. 55, iss. 8, pp. 1124–1130. DOI: [10.1134/S0016793215080125](https://doi.org/10.1134/S0016793215080125).
- Kennewell J.A. 18th NSO/Sacramento Peak Summer Workshop “Synoptic Solar Physics”. Sunspot, New Mexico, 8–12 September 1997. *ASP Conf. Ser.* 1998, vol. 140, pp. 529.
- Knipp D.J., Ramsay A.C., Beard E.D., et al. The May 1967 great storm and radio disruption event: Extreme space weather and extraordinary responses. *Space Weather*. 2016, vol. 14, iss.9, pp. 614–633. DOI: [10.1002/2016SW001423](https://doi.org/10.1002/2016SW001423).
- Kosugi T., Matsuzaki K., Sakao T., Shimizu, T., Sone Y., Tachikawa S., et al. The Hinode (Solar-B) Mission: An Overview. *Solar Phys.* 2007, vol. 243, iss.1, pp. 3–17. DOI: [10.1007/s11207-007-9014-6](https://doi.org/10.1007/s11207-007-9014-6).
- Krieger A.S., Timothy A.F., Roelof E.C. A coronal hole and its identification as the source of a high velocity solar wind stream. *Solar Phys.* 1973, vol. 29, iss. 2, pp. 505–525. DOI: [10.1007/BF00150828](https://doi.org/10.1007/BF00150828).
- Kuznetsov A.A., Kontar E.P. Spatially resolved energetic electron properties for the 21 May 2004 flare from radio observations and 3D simulations. *Solar Phys.* 2015, vol. 290, iss. 1, pp. 79–93. DOI: [10.1007/s11207-014-0530-x](https://doi.org/10.1007/s11207-014-0530-x).
- Lesovoi S.V., Kobets V.S. Correlation dependences of the Siberian Radioheliograph. *Solar-Terr. Phys.* 2017, vol. 3, iss. 1, pp. 19–25. DOI: [10.12737/article_58f96eeb8fa318.06122835](https://doi.org/10.12737/article_58f96eeb8fa318.06122835).
- Lesovoi S.V., Kobets V.S. Simulating Siberian Radioheliograph response to the quiet Sun. *Solar-Terr. Phys.* 2018, vol. 4, iss. 4, pp. 82–87. DOI: [10.12737/stp-44201811](https://doi.org/10.12737/stp-44201811).
- Lesovoi S.V., Altyntsev A.T., Ivanov E.F., Gubin A.V. The Multifrequency Siberian Radioheliograph. *Solar Phys.* 2012, vol. 280, iss. 2, pp. 651–661. DOI: [10.1007/s11207-012-0008-7](https://doi.org/10.1007/s11207-012-0008-7).
- Lesovoi S.V., Altyntsev A.T., Ivanov E.F., Gubin A.V. A 96-antenna radioheliograph. *Res. Astron. Astrophys.* 2014, vol. 14, iss. 7, pp. 864–868. DOI: [10.1088/1674-4527/14/7/008](https://doi.org/10.1088/1674-4527/14/7/008).
- Lesovoi S.V., Altyntsev A.T., Kochanov A.A., Grechnev V.V., Gubin A.V., Zhdanov D.A., et al. Siberian Radio Heliograph: First Results. *Solar-Terr. Phys.* 2017, vol. 3, iss. 1, pp. 3–18. DOI: [10.12737/article_58f96ec60fec52.86165286](https://doi.org/10.12737/article_58f96ec60fec52.86165286).
- Maksimov V.P., Bakunina I.A., Nefedyev V.P., Smolkov G.Ya. Method of short-term forecast of powerful solar flares. *Patent N 2114449 ot 27.06.1998. Byulleten' izobretenii [Bull. Inventions]*. 1996, vol. 21, pp. 131–134. (In Russian).
- Maksimov V.P., Prosovetsky D.V. Structure of the program of short-term prediction of power solar flares. *Chin. J. Space Sci. (Spec. Iss.)*. 2005, vol. 25, iss. 5, pp. 329–332.
- Marqué C., Klein K.-L., Monstein C., **Opgenoorth H, Pulkkinen A, Buchert S.**, et al. Solar radio emission as a disturbance of aeronautical radionavigation. *J. Space Weather and Space Climate*. 2018, vol. 8, id. A42, 13 p.
- Muratov A.A. Solar spectropolarimeter for 2–8 GHz range. *Baikal Young Scientists' International School on Fundamental Physics. XII Young Scientists' Conference "Interaction of Fields and Radiation with Matter"*. Irkutsk, September 19–24, 2011, pp. 21–22. (In Russian).
- Nakajima H., Sekiguchi H., Sawa M., Kai K., Kawashima S. The radiometer and polarimeters at 80, 35, and 17 GHz for solar observations at Nobeyama. *Publ. Astron. Soc. Japan*. 1985, vol. 37, no. 1, p. 163.
- Nakajima H., Nishio M., Enome S., Shibasaki K., Takano T., Hanaoka Y., et al. The Nobeyama radioheliograph. *Proc. IEEE*. 1994, vol. 82, iss. 5, pp. 705–713.
- Pesnell W.D., Thompson B.J., Chamberlin P.C. The Solar Dynamics Observatory (SDO). *Solar Phys.* 2012, vol. 275, iss. 1-2, pp. 3–15. DOI: [10.1007/s11207-011-9841-3](https://doi.org/10.1007/s11207-011-9841-3).
- Rudenko G.V., Myshyakov I.I. Analysis of reconstruction methods for nonlinear force-free fields. *Solar Phys.* 2009, vol. 257, iss.2, pp. 287–304. DOI: [10.1007/s11207-009-9389-7](https://doi.org/10.1007/s11207-009-9389-7).
- Schonfeld S.J., White S.M., Henney C.J., Arge C.N., McAteer R.T.J. Coronal sources of the solar F10.7 radio flux. *Astrophys. J.* 2015, vol. 808, iss. 1, article id. 29, 10 p. DOI: [10.1088/0004-637X/808/1/29](https://doi.org/10.1088/0004-637X/808/1/29).
- Shibasaki K. Long-term global solar activity observed by the Nobeyama Radioheliograph. *Publ. Astron. Soc. Japan*. 2013, vol. 65, iss. SP1, S17. DOI: [10.1093/pasj/65.sp1.S17](https://doi.org/10.1093/pasj/65.sp1.S17).
- Smolkov G.Ya., Uralov A.M., Bakunina I.A. Radioheliographic diagnostics of the potential flare productivity of active regions. *Geomagnetism and Aeronomy*. 2009, vol. 49, pp. 1101–1105. DOI: [10.1134/S0016793209080106](https://doi.org/10.1134/S0016793209080106).
- Smolkov G.Ya., Maksimov V.P., Prosovetskii D.V., Uralov A.M., Bakunina I.A. An experience of radioheliographic prediction of powerful solar flares. *Bull. Crimean Astrophys. Observatory*. 2010, vol. 106, pp. 31–33. DOI: [10.3103/S0190271710010055](https://doi.org/10.3103/S0190271710010055).
- Smolkov G.Ya., Pistolkors A.A., Treskov T.A., Krissinel B.B., Putilov V.A., Potapov N.N. The Siberian Solar Radio-Telescope: Parameters and principle of operation, objectives and results of first observations of spatio-temporal properties of development of active regions and flares. *Astrophys. Space Sci.* 1986, vol. 119, iss. 1, pp. 1–4. DOI: [10.1007/BF00648801](https://doi.org/10.1007/BF00648801).
- Stenflo J.O. Stokes polarimetry of the Zeeman and Hanle effects. *ISSI Scientific Rep. Ser.* 2010, vol. 9, pp. 543–557.
- Tanaka H., Enome S. The microwave structure of coronal condensations and its relation to proton flares. *Solar Phys.* 1975, vol. 40, pp. 123–131. DOI: [10.1007/BF00183156](https://doi.org/10.1007/BF00183156).
- Tokhchukova S., Bogod V.M. Detection of long-term microwave “darkening” before the 14 July 2000 flare. *Solar Phys.* 2003, vol. 212, pp. 99–109. DOI: [10.1023/A:1022967619993](https://doi.org/10.1023/A:1022967619993).
- Torii C., Tsukiji Y., Kobayashi S., Yoshimi N., Tanaka H., Enome S. Full-automatic radiopolarimeters for solar patrol at microwave frequencies. *Proc. Research Institute of Atmospheric and Space Sciences, Nagoya University*. 1979, vol. 26, p. 129.
- Treumann R.A. The electron-cyclotron maser for astrophysical application. *Astron. Astrophys. Rev.* 2006, vol. 13, pp. 229–315. DOI: [10.1007/s00159-006-0001-y](https://doi.org/10.1007/s00159-006-0001-y).
- Tritschler A., Rimmele T.R., Berukoff S., Casini R., Kuhn J.R., Lin H., Rast M.P., Mc-Mullin J.P., Schmidt W., Wöger F., DKIST Team, Daniel K. Inouye Solar Telescope: High-resolution observing of the dynamic Sun. *Astronomische Nachrichten*. 2016, vol. 337, p. 1064. DOI: [10.1002/asna.201612434](https://doi.org/10.1002/asna.201612434).
- Tsurutani B.T., Gonzalez W.D., Gonzalez A.L.C., Guarnieri F.L., Gopalswamy N., Grande M., et al. Corotating solar wind streams and recurrent geomagnetic activity: A review. *J. Geophys. Res.* 2006, vol. 111, no. A07S01. DOI: [10.1029/2005JA011273](https://doi.org/10.1029/2005JA011273).
- Tsurutani B.T., Verkhoglyadova O.P., Mannucci A.J., Lakhina G.S., Li G., Zank G.P. A brief review of solar flare effects on the ionosphere. *Radio Sci.* 2009, vol. 44, RS0A17. DOI: [10.1029/2008RS004029](https://doi.org/10.1029/2008RS004029).
- Uralov A.M., Rudenko I.G. 17 GHz neutral line associated sources: birth, motion, and projection effect. *Publ. Astron. Soc. Japan*. 2006, vol. 58, p. 21. DOI: [10.1093/pasj/58.1.21](https://doi.org/10.1093/pasj/58.1.21).
- Uralov A.M., Grechnev V.V., Rudenko G.V., Rudenko I.G., Nakajima H. Microwave neutral line associated source and a current sheet. *Solar Phys.* 2008, vol. 249, pp. 315–335. DOI: [10.1007/s11207-008-9183-y](https://doi.org/10.1007/s11207-008-9183-y).
- Wang Z., Gary D.E., Fleishman G.D., White S.M. Coronal magnetography of a simulated solar active region from microwave imaging spectropolarimetry. *Astrophys. J.* 2015, vol. 805, iss. 2, article id. 93, 13 p. DOI: [10.1088/0004-637X/805/2/93](https://doi.org/10.1088/0004-637X/805/2/93).
- Yan Y., Zhang J., Wang W., Liu F., Chen Z., Ji G. The

Chinese Spectral Radioheliograph — CSRH. *Earth, Moon, and Planets*. 2009, vol. 104, iss. 1-4, pp. 97–100. DOI: [10.1007/s11038-008-9254-y](https://doi.org/10.1007/s11038-008-9254-y).

Yasyukevich Y., Astafyeva E., Padokhin A., Ivanova V., Syrovatskii S., Podlesnyi A. The 6 September 2017 X-class solar flares and their impacts on the ionosphere, GNSS and HF radio wave propagation. *Space Weather*. 2018, vol. 16, pp. 1013–1027. DOI: [10.1029/2018SW001932](https://doi.org/10.1029/2018SW001932).

Yaya P., Hecker L., Dudok de Wit T., le Fèvre C., Bruinsma S. Developing new space weather tools: Transitioning fundamental science to operational prediction systems. *J. Space Weather Space Climate*. 2017, vol. 7, iss. A35. DOI: [10.1051/swsc/2017032](https://doi.org/10.1051/swsc/2017032).

Zhang J., Richardson I.G., Webb D.F., Gopalswamy N., Huttunen E., Kasper J.C., Nitta N.V., Poomvises W., Thompson B.J., Wu C.-C., Yashiro S., Zhukov A.N. Solar and interplanetary sources of major geomagnetic storms ($Dst \leq -100$ nT) during 1996–2005. *J. Geophys. Res.* 2007, vol. 112, iss. A10, citeID A10102. DOI: [10.1029/2007JA012321](https://doi.org/10.1029/2007JA012321).

Zhdanov D.A., Zandanov V.G. Observations of microwave fine structures by the Badary Broadband Microwave Spectropolarimeter and the Siberian Solar Radio Telescope. *Solar Phys*. 2015, vol. 290, iss. 1, pp. 287–294. DOI: [10.1007/s11207-014-0553-3](https://doi.org/10.1007/s11207-014-0553-3).

URL: <http://badary.iszf.irk.ru/srhCorrPlot.php> (accessed October 20 2019).

URL: <https://www.ngdc.noaa.gov> (accessed October 20 2019).

URL: <https://solar.nro.nao.ac.jp/norp> (accessed September 20 2019).

URL: <http://ckp-rf.ru/usu/73606> (accessed September 20 2019).

How to cite this article

Altyntsev A.T., Lesovoi S.V., Globa M.V., Gubin A.V., Kochanov A.A., Grechnev V.V., Ivanov E.F., Kobets V.S., Meshalkina N.S., Muratov A.A., Prosovetsky D.V., Myshyakov I.I., Uralov A.M., Fedotova A.Yu. Multiwave Siberian Radioheliograph. *Solar-Terrestrial Physics*. 2020. Vol. 6. Iss. 2. P. 30–40. DOI: [10.12737/stp-62202003](https://doi.org/10.12737/stp-62202003).